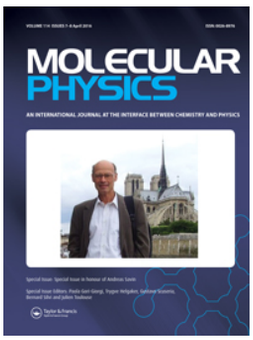

Taylor & Francis
Taylor & Francis Group

Molecular Physics

An International Journal at the Interface Between Chemistry and Physics

ISSN: 0026-8976 (Print) 1362-3028 (Online) Journal homepage: http://www.tandfonline.com/loi/tmph20

Accurate atomic quantum defects from particle–particle random phase approximation

Yang Yang, Kieron Burke & Weitao Yang

To cite this article: Yang Yang, Kieron Burke & Weitao Yang (2016) Accurate atomic quantum defects from particle–particle random phase approximation, Molecular Physics, 114:7-8, 1189-1198, DOI: 10.1080/00268976.2015.1123316

To link to this article: https://doi.org/10.1080/00268976.2015.1123316

MOLECULAR PHYSICS, 2016
VOL. 114, NOS. 7–8, 1189–1198
http://dx.doi.org/10.1080/00268976.2015.1123316

Taylor & Francis
Taylor & Francis Group

INVITED ARTICLE

Accurate atomic quantum defects from particle–particle random phase approximation

Yang Yang [a], Kieron Burke[b] and Weitao Yang[a,c,d]

[a]Department of Chemistry, Duke University, Durham, NC, USA; [b]Department of Chemistry, University of California, Irvine, CA, USA; [c]Department of Physics, Duke University, Durham, NC, USA; [d]Key Laboratory of Theoretical Chemistry of Environment, Ministry of Education, School of Chemistry and Environment, South China Normal University, Guangzhou, China

ABSTRACT

The accuracy of calculations of atomic Rydberg excitations cannot be judged by the usual measures, such as mean unsigned errors of many transitions. We show how to use quantum defect (QD) theory to (a) separate errors due to approximate ionisation potentials, (b) extract smooth QDs to compare with experiment, and (c) quantify those defects with a few characteristic parameters. The particle–particle random phase approximation (pp-RPA) produces excellent Rydberg transitions that are an order of magnitude more accurate than those of time-dependent density functional theory with standard approximations. We even extract reasonably accurate defects from the lithium Rydberg series, despite the reference being open-shell. Our methodology can be applied to any Rydberg series of excitations with four transitions or more to extract the underlying threshold energy and characteristic QD parameters. Our pp-RPA results set a demanding challenge for other excitation methods to match.

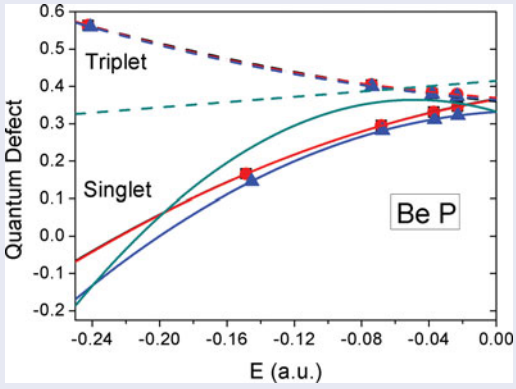

ARTICLE HISTORY
Received 28 October 2015
Accepted 16 November 2015

KEYWORDS
Quantum defect; Rydberg excitation; particle–particle random phase approximation

1. Introduction

An accurate description of electronic excited states has always been a major goal for theoretical and computational chemists. Nowadays, linear-response time-dependent density functional theory (LR-TDDFT) [1–4] has become the standard workhorse for practical applications, because of the favorable balance between accuracy and computational cost. However, there are a variety of well-established limitations of TDDFT with the standard semilocal functionals [5]. These challenges include double excitations, charge transfer (CT) excitations, and Rydberg excitations [4,6–10]. Although many of these problems can be ameliorated by using range-separated [11,12] or more accurate asymptotic-corrected response kernels [13–16], the results are not always satisfactory, and a more careful examination beyond the usual tabulations of mean absolute errors is required to check for an accurate Rydberg series.

Quantum defect (QD) theory [17] has long been applied as a test for atomic Rydberg excitations [18]. In the long history of quantum mechanics, the QD was originally introduced to empirically describe weak electron penetration effects relative to strong shielding effect [17,19]. Later, systematic derivations were given, creating

CONTACT Yang Yang yy88@duke.edu
Supplemental data for this article can be accessed at: http://dx.doi.org/10.1080/00268976.2015.1123316.

a non-empirical theory [17]. The QD can also be applied to describe many molecular Rydberg states [20–24]. Al-Sharif *et al.* [25] first pointed out that the exact ground-state Kohn–Sham potential yields QDs that are an excellent starting point for approximations.

In the present work, we restrict ourselves to atomic Rydberg series. QDs are often given as lists, with the index corresponding to the principal quantum number. But the crucial feature of QDs is that they are smoothly varying functions of the energy. In fact, they even merge continuously with scattering phase shifts across the ionisation threshold [26]. We use the smoothness feature to create our procedure for extracting QDs from lists of excitation energies. In earlier work, van Faassen and Burke [18] analysed the singlet and triplet spin-states of the S- and P- series for atomic helium, beryllium, and neon as test cases for standard TDDFT. Although excitation energy errors were no more than a few millihartrees, the delicate QD results exposed their limitations. With a ground-state density functional theory (DFT) calculation that yields a potential with the correct asymptotic decay (although see Ref. [27] for a way around even this restriction), QDs that were reasonably but not highly accurate were usually found with semilocal approximations to the kernel in TDDFT. Later, the D series in Be was shown to be very poorly described by TDDFT [28].

The particle–particle random phase approximation (pp-RPA) has long been a textbook method for treating correlation in nuclear physics [29,30]. Recently, it was introduced by van Aggelen *et al.* to atomic and molecular systems for correlation energy calculations [31], and was combined with DFT as well as the conventional Hartree–Fock (HF) theory. The pp-RPA correlation energy calculation with a HF reference was subsequently shown to be equivalent to ladder-coupled-cluster doubles [32,33]. A more comprehensive benchmark test based on both DFT and HF references was followed [34]. The pp-RPA had also been applied to the calculation of Auger spectroscopy for molecules [35,36], which involves a two-electron removal process, but it had never been previously applied to particle-number conserving excitations. Recently, two of us applied the pp-RPA and the particle–particle Tamm-Dancoff approximation (pp-TDA) theories to such challenging excitations as double excitations, CT excitations, Rydberg excitations, and excitations in diradicals [37–39]. Good excitation energies were typically found with a relatively low $O(N^4)$ computational cost, where N is the number of virtual orbitals [38]. Furthermore, the pp-RPA has also been derived from a linear response perspective [40]. It describes the pairing matrix response to a pairing field. Therefore, it is a parallel counterpart to the conventional LR-TDDFT, which describes the density matrix response to a local normal potential field. Thus, pp-RPA and pp-TDA are promising methods that complement standard LR-TDDFT, especially for those aforementioned challenging cases. In the present work, we develop the QD analysis to more stringently test pp-RPA and pp-TDA of Rydberg excitations, and compare them to TDDFT.

Table 1. First 11 excitation energies (in Hartree) in Be ^{1}P series and their mean signed/unsigned error (MSE/MUE).

Transition	Expt.	pp-TDA	ALDA
2s→2p	0.1940	0.1959	0.1868
2s→3p	0.2742	0.2737	0.2710
2s→4p	0.3054	0.3047	0.3048
2s→5p	0.3195	0.3186	0.3194
MSE (mH)		−0.1	−2.8
MUE (mH)		1.1	2.8
2s→6p	0.3269	0.3259	0.3269
2s→7p	0.3313	0.3302	0.3313
2s→8p	0.3340	0.3329	0.3341
2s→9p	0.3359	0.3348	0.3359
2s→10p	0.3372	0.3361	0.3372
2s→11p	0.3382	0.3370	0.3382
2s→12p	0.3389	0.3378	0.3389
MSE (mH)		−1.1	0.0
MUE (mH)		1.1	0.0
All			
MSE (mH)		−0.7	−1.0
MUE (mH)		1.1	1.0

Notes: For transitions to $n = 6$ and higher, the values have been extracted from the fits to the associated QDs given later (for ALDA, this begins at $n = 5$).

To illustrate the need for the QD analysis, we first analyze a Rydberg series using the traditional methods of measuring errors in electronic structure methods. In Table 1, we list the lowest 11 excitation energies in the Be P singlet series. We include the experimental values, the pp-TDA results (details given later), and TDDFT calculations using the adiabatic local density approximation (ALDA) kernel and *exact* ground-state KS potential (see Ref. [18]). We see that, for the lowest transition frequencies, pp-TDA is far better than ALDA. But beyond about the fifth transition, the pp-TDA error stops decreasing, while the ALDA error keeps getting smaller. Thus, when we average over transitions 2–5, pp-TDA is clearly much better than ALDA. But when average over 6–12, the order has been reversed, so that ALDA now appears better when averaged over all transitions. This trend would continue, with the mean errors in ALDA going to zero as the total number of transitions included increases, while that of pp-TDA tends to about 1 mH. However, we show below that this is entirely an artefact of the error in the ionisation potential (IP) of pp-TDA, which is absent in the TDDFT calculations by virtue of using the exact KS potential. As the number of transitions included increases, the errors reflect simply the error in the IP. For any finite number,

there is no way to separate the two effects by this means. In fact, we show below that the pp-TDA results listed here are almost an order of magnitude better than the TDDFT results.

2. Theory

2.1. Quantum defect theory as a measure of Rydberg excitations

Consider a Rydberg series of excited states of a neutral atom, with energies $E_{l,S}(n)$ below the ionisation threshold, where n runs from the first allowed excitation and is unbounded. The QD for this series is defined by:

$$E_{l,S}(n) = -\frac{1}{2(n-\mu_{l,S}(n))^2}, \tag{1}$$

i.e. as n grows, E approaches 0 ever more slowly, mimicking the behaviour of a H-atom series, but with small deviations. The QD is a dimensionless measure of the deviation from a pure hydrogenic series.

The key ingredient of our analysis is to generalise the QD as a function of index n to a continuous function of E, i.e. $\mu(E)$ [18,28], with the requirement that

$$\mu(n) = \mu(E(n)). \tag{2}$$

In fact, all QDs are smooth functions of E in practice. We make the further assumption that, on the scale of energies spanned by the series, μ is not strongly varying, and can usually be well-approximated by a simple parabola:

$$\mu(E) \approx a + bE + cE^2. \tag{3}$$

Thus an entire, infinite Rydberg series can be very accurately represented by three real numbers, one of which (a) is simply the QD at threshold μ_0, and the accuracy of an approximate Rydberg series can be judged by the accuracy of its approximation for a, b, c. For the rest of this paper, we approximate all such curves by parabolas.

But transition frequencies are measured or calculated relative to the ground state, so a fourth number, the IP, enters:

$$\omega_n = I - \frac{1}{2(n-\mu_n)^2}, \tag{4}$$

or

$$\mu_n = n - \frac{1}{\sqrt{2(I-\omega_n)}}. \tag{5}$$

While I might be known very accurately for a given experiment, in calculations its precise value is slightly affected by the limitations of a calculation, such as finite basis sets. As n grows, even tiny errors in I will cause μ_n to become highly inaccurate. Thus our procedure is designed to accommodate uncertainty in the value of I, and below we test this in cases where I is known.

Expanding $\mu(E)$ in a Taylor series around $E = 0$, we find

$$\omega_n = I - [2(x - (\tilde{b} - \tilde{c}/(2x^2)/(2x^2)]^{-1}, \quad x = n - \tilde{a}. \tag{6}$$

Thus, given at least four transition frequencies, we can fit a Rydberg series to find the best four parameters, which gives us our best estimate for I. Note that we have added a tilde to each of a, b, c, because these parameters are *not* best estimated by this procedure, as we performed an expansion around $E = 0$ to find Equation (6). Thus, in a second fitting step, we fix I, and refit a, b, c via Equations (3)–(5), yielding our best estimate for these. Once we have values for a, b, c, we plot the QD as a function of E and see how well a method performs.

A final piece of methodology is to convert the parameters a, b, c to others that are easier to interpret. Denote by E_m the minimum value of E, i.e, the lowest transition in the series. We then write

$$\mu(E) = \mu_0 + x\,\Delta\mu + 4x(1-x)\,\Delta^2\mu, \quad x = E/E_m. \tag{7}$$

The parameters have been carefully chosen to have an immediate physical interpretation. Here μ_0 is the QD at threshold, while $\Delta\mu$, the QD shift, is the change in QD from the lowest transition to the threshold. A negative value means the QD drops, a positive value means it is rising, and $\mu_0 + \Delta\mu$ is the fit value of $\mu(E_m)$. Lastly, we call $\Delta^2\mu$ the QD curvature, and is the maximum deviation from linearity, which occurs at $E_m/2$. A negative value means the curve is convex, a positive value means it is concave. This simple geometric interpretation is shown in Figure 1. We will use these values to judge and interpret the accuracy of approximate calculations of Rydberg series.

2.2. Basic theory on pp-RPA

The pp-RPA can be derived in a variety of independent ways, including via the adiabatic connection-pairing matrix fluctuations [31,41], equations of motion [29,34,42], and time-dependent density functional theory with a pairing field (TDDFT-P) [40]. The key working

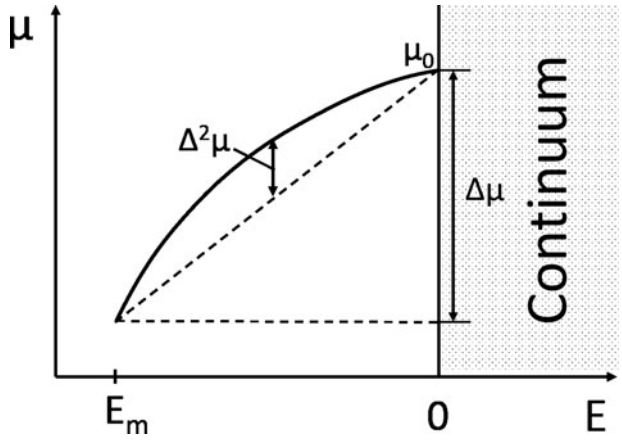

Figure 1. Geometric illustration of the physical meanings of QD parameters.

equation of pp-RPA is a generalised eigenvalue equation

$$\begin{bmatrix} \mathbf{A} & \mathbf{B} \\ \mathbf{B}^\dagger & \mathbf{C} \end{bmatrix} \begin{bmatrix} \mathbf{X} \\ \mathbf{Y} \end{bmatrix} = \omega^{N\pm 2} \begin{bmatrix} \mathbf{I} & \mathbf{0} \\ \mathbf{0} & -\mathbf{I} \end{bmatrix} \begin{bmatrix} \mathbf{X} \\ \mathbf{Y} \end{bmatrix}, \tag{8}$$

with

$$\begin{aligned} A_{ab,cd} &= \delta_{ac}\delta_{bd}(\epsilon_a + \epsilon_b) + \langle ab||cd\rangle \\ B_{ab,kl} &= \langle ab||kl\rangle \\ C_{ij,kl} &= -\delta_{ik}\delta_{jl}(\epsilon_i + \epsilon_j) + \langle ij||kl\rangle, \end{aligned} \tag{9}$$

where a, b, c, d are virtual orbital indices and i, j, k, l are occupied orbital indices with the restrictions that $a > b$, $c > d$, $i > j$, and $k > l$. The brackets are defined as

$$\langle pq|rs\rangle \equiv \int d\mathbf{r}_1 d\mathbf{r}_2 \frac{\phi_p^*(\mathbf{r}_1)\phi_q^*(\mathbf{r}_2)\phi_r(\mathbf{r}_1)\phi_s(\mathbf{r}_2)}{|\mathbf{r}_1 - \mathbf{r}_2|}, \tag{10}$$

and $\langle pq||rs\rangle \equiv \langle pq|rs\rangle - \langle pq|sr\rangle$. This equation describes the transition process of adding or removing *two* electrons from a system. In an excitation energy calculation, we usually adopt a two-electron deficient reference and investigate its two-electron addition processes, yielding a series of neutral states including both the ground and electronically excited states. Differences between transition energies are neutral excitation energies with

$$E^N_{0\to n} = \left(E^N_n - E^{N-2}_0\right) - \left(E^N_0 - E^{N-2}_0\right), \tag{11}$$

where N and $N-2$ denote the number of electrons, and 0 and n denote the ground and excited states, respectively. By solving Equation (8) and processing the output with Equation (11), we obtain the excitation energies for the N-electron system.

There is a corresponding pp-TDA to pp-RPA. We simply set $\mathbf{B} = \mathbf{C} = 0$. The result of pp-TDA is often similar to pp-RPA, and the difference is negligible in small systems with limited number of electrons. Therefore, we use the pp-TDA throughout this paper, which is slightly cheaper than pp-RPA.

3. Computational details

We choose both singlet (S=0) and triplet (S=1) Rydberg series for all our tests, so we are probing both spin-conserving and spin-flipping excitations with respect to the ground state. We look at three different angular momenta: S, P, D, to further test the pp-RPA method. Lastly, we consider two different closed-shell atoms, Be and Mg, whose QDs are very distinct, and also apply our methods to Li, to see the challenges of an open-shell ground state. The difference between pp-TDA and pp-RPA is almost undetectable for these species, so we report data computed with pp-TDA. We use HF for the reference. A very extensive even-tempered basis set was built [43,44] with exponents satisfying $\alpha_i = \alpha_1 \beta^{i-1}$. Each basis contains 22s, 18p, and 17d functions with the smallest exponents being $\alpha_1 = 0.0002441406$, 0.0004882813, and 0.0002441406, respectively. The basis has been tested to give highly converged excitation energies ($\Delta E < 0.1$ mH) for diffuse Rydberg states as high as $n = 6$. All calculations are performed with Cartesian basis set on the QM4D package [45].

4. Results

In this section, we systematically dissect the results of our calculations.

4.1. Extracting ionisation potentials

Since the IP of a given, calculated Rydberg series is often not reported (or possibly not even calculated), in this section we demonstrate that our fitting procedure provides a method for *extracting* accurate IPs from such a series.

We do this by applying our procedure to the *experimental* transition frequencies, and comparing the fitted IP with the experimental value. The IPs of Be and Mg are 0.342603 and 0.280994 Hartree, respectively [46]. For both Be and Mg, we have six separate Rydberg series, and for Li we have three. In Table 2, we list all the errors in the IPs extracted from the fitting procedure. In the rows marked Exp, we have fitted the IP in each Rydberg series, and measure the error relative to the exact value. We see that errors are of order 0.05 mH or less, showing how accurately the IP can be found from a Rydberg series.

The error in the averaged IPs from the series is only 2×10^{-5} H, which is around 5×10^{-4} eV. These results not only confirm the validity of our fit, but also show the magic of QD theory. With only four accurate data points

Table 2. Errors (in mH) in fitted ionisation potential for Be and Mg Rydberg series.

		^{1}S	^{1}P	^{1}D	^{3}S	^{3}P	^{3}D	Avg
Expt.	Be	0.011	− 0.008	− 0.006	0.024	0.073	0.032	0.021
	Mg	− 0.005	− 0.003	− 0.034	0.025	0.052	0.017	0.009
pp	Be	− 1.057	− 1.173	− 0.958	− 1.053	− 1.002	− 1.038	− 1.047
	Mg	− 5.172	− 5.148	− 5.130	− 5.174	− 5.102	− 5.161	− 5.148

Note: Expt. is experimental series; pp is the pp-TDA calculation with HF reference; and Avg is the average of all six estimated IPs.

Table 3. Same as Table 2 but for Li doublet series.

	S	P	D	Avg
Expt.	0.010	0.010	0.007	0.009
pp-AB	4.203	4.237	4.230	4.223
pp-BB	− 3.252	− 3.219	− 3.225	− 3.232
pp-AVE	0.476	0.509	0.502	0.496

in a Rydberg series, QD theory yields an IP of this accuracy. Furthermore, in principle, if we plug the acquired parameters (a, b, c, and IP) to Equation (6), we can predict all the excitation energies in that Rydberg series.

In the second set of IPs, we see the values from the pp calculation. Now we can see that the average IP differs noticeably from the experimental value (−1 mH for Be, −5 mH for Mg). This reflects the error in the IP of the underlying reference HF calculation. But given this built-in error, we see that the pp Rydberg series are extremely consistent. None differ by more than 0.1 mH from the average value. Thus, QD analysis is extracting the underlying IP to within 0.1 mH, i.e. it shows that the IP for the Be reference calculation is 0.3416 Hartree, and for Mg it is 0.2759 Hartree.

In Table 3, we give the results for the extremely challenging case of Li. The exact IP is 0.198142 Hartree [46]. Now we can see that each of the calculated series AB and BB (details given later) has its own distinct ionisation threshold, each with noticeable errors. However, when we average over transition frequencies, the new series (AVE) has a much more accurate ionisation threshold, suggesting that is a good way to deal with the open-shell issue. In fact, every transition energy of the AVE series is better than the corresponding energy of either AB or BB.

4.2. QD errors due to fitting

In this section, we extract the QD parameters for the experimental Rydberg series, using the known IPs, and also consider the calculated parameters when the IP is fitted. This gives us a measure of the error introduced into the calculated QDs due to that fitting.

In Table 4, we give the parameters for all the different Rydberg series examined in this paper, using the experimental data. The first point to notice is the value of the QD at threshold. These vary from about 1.6 down to about −0.1. These dimensionless numbers are very important, as knowing only this value often yields a reasonably accurate Rydberg series, and also determines the scattering cross-section in the low-energy limit [47]. It is clear that our series cover a large range of different values for the QD.

Table 4. QD parameters (times 100) obtained from experimental Rydberg series, both with and without experimental IP value.

	Expt. IP			Fit IP		
tr.	μ_0	$\Delta\mu$	$\Delta^2\mu$	μ_0	$\Delta\mu$	$\Delta^2\mu$
			Be			
1S	67.1	− 1.6	0.1	67.4	− 1.3	0.2
3S	77.2	− 4.9	− 0.0	77.8	− 4.3	0.2
1P	36.7	20.1	− 2.1	36.6	20.0	− 2.1
3P	36.0	− 20.4	2.2	37.0	− 19.4	2.9
1D	− 10.2	9.2	− 1.9	− 10.4	8.9	− 2.0
3D	10.4	− 0.6	− 0.2	11.6	0.6	0.2
MSE				0.4	0.4	0.2
MUE				0.6	0.5	0.3
			Mg			
1S	152.0	− 2.2	0.1	152.2	− 2.0	0.2
3S	162.4	− 6.1	0.0	162.6	− 5.8	0.1
1P	104.6	7.6	− 0.5	104.7	7.8	− 0.5
3P	112.5	− 21.5	1.9	112.7	− 21.3	2.0
1D	60.3	28.4	3.1	60.6	28.7	3.2
3D	16.6	− 0.5	0.0	16.9	− 0.2	0.1
MSE				0.2	0.2	0.1
MUE				0.2	0.2	0.1
			Li			
2S	39.6	− 0.7	− 0.1	39.9	− 0.5	− 0.0
2P	4.5	0.5	− 0.1	4.7	0.6	− 0.0
2D	− 0.2	− 0.3	− 0.1	0.1	0.0	− 0.0
MSE				0.3	0.3	0.1
MUE				0.3	0.3	0.1

Next, consider the values of $\Delta\mu$. These can have either sign, meaning the QD can either increase or decrease with energy. The magnitude varies from almost 0 up to about 0.3. This gives the scale of the total change in the QD from the first transition to the threshold. Finally, we consider $\Delta^2\mu$. These values are much smaller, never being larger than about 0.03, but also vary in sign. Thus this measure shows that the curvature has relatively little effect on the

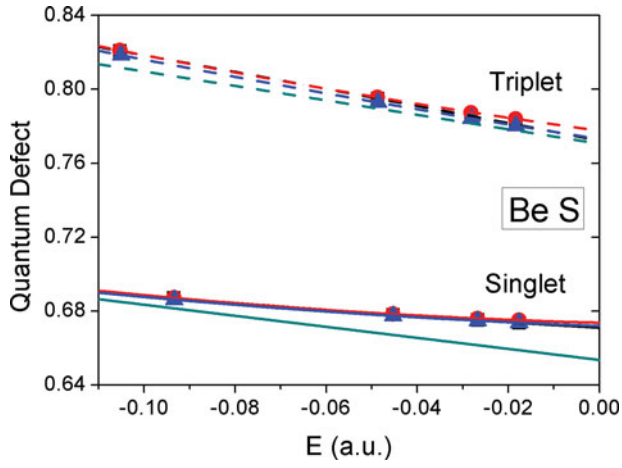

Figure 2. (Colour online) S quantum defects for atomic Be from experimental data (black square), with fitted IP (red circle), from pp-TDA (blue triangle), and from TDLDA (green without label).

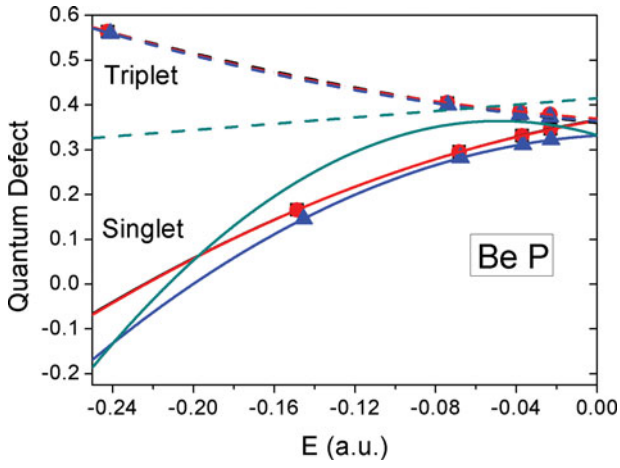

Figure 3. Same as Figure 2, but for *P*.

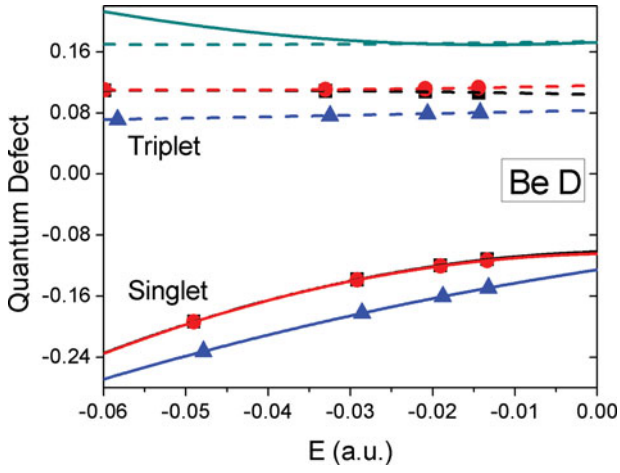

Figure 4. Same as Figure 2, but for *D*.

actual value of QD, and therefore on the Rydberg transition frequencies.

Now, we consider the values of the parameters that we found when the threshold energy was fitted rather than known from experiment. Typical errors introduced by the fitting procedure are about 0.004 or less. The only real outlier is the triplet D series in Be, where the threshold value is in error by 0.01. The curvature errors are typically even smaller (0.001), but since their values are already small, this appears as a greater fractional error. We conclude that errors on this scale will be introduced to QD parameters whenever IPs are fit, as is done for all our pp calculations in the rest of this paper. Such errors are smaller than those made by the approximations we study below.

4.3. Results for Be

We begin the presentation of results with the simplest case: singlet and triplet S excitations in Be. We plot the experimental and pp-TDA results in Figure 2, as well as the fit of TDDFT with ALDA kernel (TDLDA) results on the exact ground-state KS potential from Ref. [18]. The figure shows several basic features. First, the difference between the black lines and red lines are almost invisible on this scale, showing that fitting the IP causes little degradation of results. Second, the pp blue lines are excellent approximations to the red lines, indicating that pp-TDA produces near perfect QDs for these series. Third, the TDDFT results (green) are quite good, especially for the triplet.

To quantify the differences in these curves, we extract μ_0, $\Delta\mu$ and $\Delta^2\mu$ from each curve in Tables 4 and 5, and compare the calculations with the experiment (with the exact IP). For both the triplet and singlet, the pp-TDA values are all excellent, and that even the curvature is within the error of the fit. The TDLDA results are almost as good (they were fit linearly [18], because the curvature is so small). However, there is a significant error in the TDLDA threshold value for the singlet, as is clearly visible in the figure, and the TDLDA slope is too large.

So, does pp-RPA always produce such excellent Rydberg series? In Figures 3 and 4, we repeat the procedure

Table 5. Same as Table 4, but for approximate Be series.

	pp			ALDA		
tr.	μ_0	$\Delta\mu$	$\Delta^2\mu$	μ_0	$\Delta\mu$	$\Delta^2\mu$
1S	67.2	−1.4	0.1	65.4	−2.8	0.0
3S	77.3	−4.5	0.1	77.1	−4.1	0.0
1P	33.2	18.6	−3.7	33.3	12.4	−8.2
3P	36.4	−19.6	2.8	41.5	9.0	0.0
1D	−12.5	10.7	−0.7	17.3	−5.0	2.1
3D	8.3	1.2	0.00	17.4	0.4	0.2
MSE	−1.2	0.5	0.1	5.8	1.3	−0.7
MUE	1.4	1.0	0.6	7.5	9.0	2.1

for the P and D series. In the P case, we see that the experimental QDs have substantially greater curvature than in the S series, especially for the singlet, and that pp-RPA captures this effect well. On the other hand, TDLDA is not working nearly as well, with the sign of $\Delta\mu$ being incorrect for the triplet, and the curvature being overestimated for the singlet.

The D QD has previously been noted as being challenging [28], and here TDLDA fails entirely. The TDLDA singlet/triplet ordering is wrong, and the threshold value is incorrect by more than 0.2. We see that although the pp-RPA results are less accurate than for S or P, they are still qualitatively and even quantitatively correct. The worst error is the threshold value for the triplet, being incorrect by 0.02, again, an order of magnitude better than TDLDA. For the Be D series, pp-RPA succeeds where TDLDA fails.

Note that these are the best possible results with ALDA because the exact ground-state KS potential was used [18]. Practical applications also require an approximation to the ground-state potential. If a standard generalised gradient approximation (GGA) or hybrid is used for the ground-state calculation, TDLDA will not produce a Rydberg series. Even methods designed to enforce the correct asymptotic behaviour of the KS potential, such as the van Leeuwen-Baerends functional or asymptotically corrected methods, will typically produce terrible QDs [18]. On the other hand, methods that include exact exchange (often denoted EXX) produce excellent KS potentials, whose TDLDA performance will be comparable to that given here, but still none will do better than the TDLDA results here as a result of the exact KS potential used for ground states.

So, we can conclude that, for essentially every Be Rydberg series, pp-RPA outperforms TDLDA, even when TDLDA has been applied to the exact ground-state KS potential (and so the underlying IP is exactly right). While ALDA does remarkably well for such a low-cost calculation, it cannot compete with pp-RPA for accuracy.

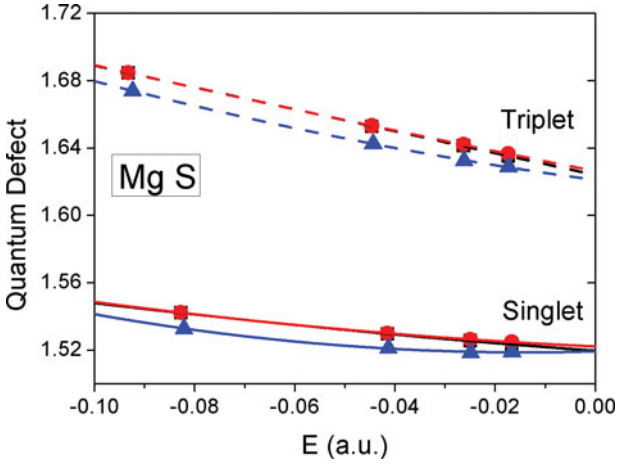

Figure 5. Same as Figure 2, but for Mg.

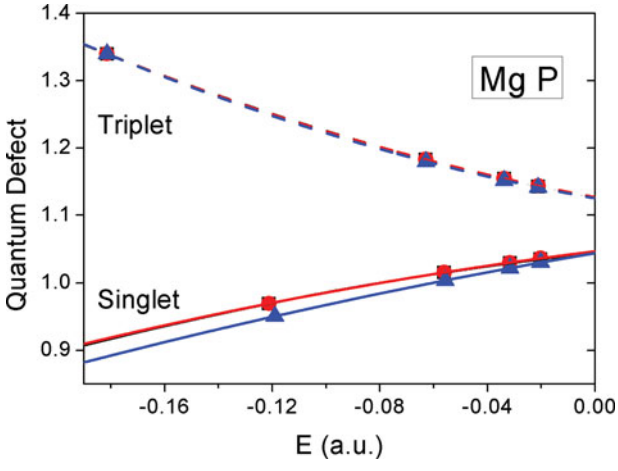

Figure 6. Same as Figure 3, but for Mg.

4.4. Results for Mg

To get an idea of how general this good performance of pp-RPA is, we repeat the calculations for Mg. The QD results are plotted in Figures 5, 6, and 7, and the QD parameters are listed in Table 6. In this case, the core is frozen leading to a substantial underestimate of the IP (0.13 eV) relative to experiment. Using the experimental

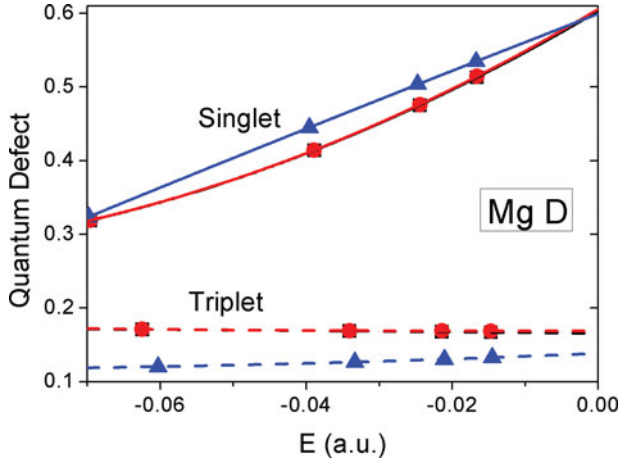

Figure 7. Same as Figure 4, but for Mg.

Table 6. Same as Table 4, but for pp Mg series.

tr.	μ_0	$\Delta\mu$	$\Delta^2\mu$
1S	151.9	−1.4	0.5
3S	162.1	−5.3	0.4
1P	104.5	9.4	−0.3
3P	112.5	−21.5	2.2
1D	59.9	27.6	−0.2
3D	13.8	1.8	0.2
MSE	−0.6	0.8	−0.3
MUE	0.6	1.1	0.8

Table 7. Same as Table 4, but for pp-TDAHF Li series.

	AB			BB			AVE		
tr.	μ_0	$\Delta\mu$	$\Delta^2\mu$	μ_0	$\Delta\mu$	$\Delta^2\mu$	μ_0	$\Delta\mu$	$\Delta^2\mu$
2S	42.2	0.1	0.2	39.3	0.1	0.2	40.7	0.1	0.2
2P	3.3	0.7	0.0	4.2	0.8	0.0	3.8	0.7	0.0
2D	0.5	0.4	0.1	0.5	0.4	0.1	0.5	0.4	0.1
MSE	0.7	0.6	0.2	0.0	0.6	0.2	0.4	0.6	0.2
MUE	1.5	0.6	0.2	0.5	0.6	0.2	0.9	0.6	0.2

IP with the pp transition frequencies would yield nonsensical QD values. But because our procedure fits this number, and then subsequent QD is plotted against the energy below threshold, we can see the Mg QD results are typically almost (not quite) as good as those for Be. When averaging over all series, the Mg results are *better* than those of Be. This is a triumph of the QD method: Despite a substantial error in IP, the QD is still extractable and the underlying error in QD is very small.

4.5. Results for an open shell

We finish our survey with an extreme challenge for pp-RPA. When the two-electron deficient reference is an unrestricted open-shell system, there are differences between α and β orbitals. The spin contamination and potential spin incompleteness usually cause both pp-RPA and pp-TDA to produce meaningless results. The lithium atom is the simplest atoms with these problems.

With an α-spin electron occupying the 1s orbital, the two-electron deficient reference for Li is hydrogenic. In principle, we can create a neutral doublet ground state by adding a β electron to 1s and another α electron to 2s, forming a $S_z = +\frac{1}{2}$ state. But we could instead add two β electrons to 1s and 2s separately to form the $S_z = -\frac{1}{2}$ state. Since we can only perform unrestricted calculations with our program, both series of excitations are spin-contaminated. We denote the two series as AB and BB.

We can also attempt to overcome spin contamination by averaging these two, denoted AVE. We try all three ways to compute the doublet S, P, and D series of Li. We saw in Section 4.1 that, since AB overestimates the IP and BB underestimates it, their average has the most accurate IP, suggesting the AVE will yield the best results for the transition energies too.

The results of all three series are shown in Figure 8 and Table 7. Note the y-scale of Figure 8 is much smaller than in previous figures, and the break in the curve. Overall, all three sets yield fairly accurate QD results, with MUEs comparable to those for Be and Mg. For the S series, the AVE QD is substantially better than either AB or BB, while for the D series, the three are indistinguishable. But for the P series, the AVE curve is definitely worse than BB. So our QD analysis has shown that, although the AVE series always has the most accurate transition energy (because of its accurate IP), it does not always produce the best QD.

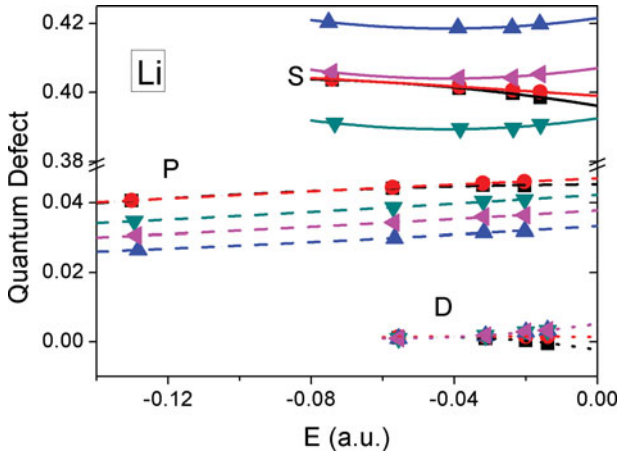

Figure 8. (Colour online) Quantum defects for atomic Li from experiment (black square), with fitted IP (red circle), from pp with AB (blue up triangle), with BB (green down triangle), and averaging (magenta left triangle). Each series (S, P, D) has a distinct line style.

4.6. Importance of pp reference state

The fact that pp-RPA and pp-TDA are able to describe CT and Rydberg excitations is often attributed to their Coulomb and exchange kernels which are asymptotically correct. However, the orbital energies from the two-electron deficient reference also play a vital role. Although the Coulomb and exchange kernel is the same, the pp-RPA and pp-TDA with DFT references substantially underestimate the Rydberg excitation energies [37] as a result of the poor Kohn–Sham orbital energies, making it meaningless to further look into the QD, just as in the TDDFT case. Because pp-RPA is only a first-order approximation to the adiabatic connection-pairing

matrix fluctuation theory, it remains sensitive to the properties of the reference calculation. A well-behaved reference, such as HF in this atomic Rydberg excitation case, is needed for pp-RPA and pp-TDA to produce meaningful QDs. However, for low-energy excitations in molecules, DFT references lead to significantly better results [38].

5. Conclusion

In this paper, we have developed a very general approach for extracting both threshold energies and QDs from limited series of Rydberg excitations. We have demonstrated that our procedure can be used to extract extremely accurate threshold energies (errors in the 0.1 mH range), and maximum errors of order 0.01 for QDs. We have shown why measures like mean unsigned errors in collections of transition frequencies are not useful for Rydberg series, and how to parametrise and quantify errors in QDs. We find that pp-RPA with a HF reference greatly outperforms TDDFT with a local approximation to the exchange-correlation kernel.

The results reported here should become the benchmark for approximate calculations of Rydberg series. Our QD extraction procedure can be applied to other series, such as excitations in solids. Any quantum chemical method for excitations should be measured against our pp-RPA results for these atoms. We suspect they will be difficult be beat with the same level of generality and low computational cost.

Acknowledgments

We dedicate this article to Andreas Savin, whose many deep insights and great papers on density functional theory have inspired us over the years. Y.Y. appreciates the support as part of the Center for the Computational Design of Functional Layered Materials, an Energy Frontier Research Center funded by the U.S. Department of Energy, Office of Science, Basic Energy Sciences under Award DE-SC0012575. K.B. was supported by the U.S Department of Energy (DOE), Office of Science, Basic Energy Sciences (BES) under award DE-FG02-08ER46496. W.Y. was supported by the National Science Foundation (CHE-1362927).

Disclosure statement

No potential conflict of interest was reported by the authors.

Funding

Center for the Computational Design of Functional Layered Materials, an Energy Frontier Research Center funded by the U.S. Department of Energy, Office of Science, Basic Energy Sciences [Grant Number DE-SC0012575]; U.S Department of Energy (DOE), Office of Science, Basic Energy Sciences (BES) [Grant Number DE-FG02-08ER46496]; National Science Foundation [Grant number CHE-1362927].

ORCID

Yang Yang http://orcid.org/0000-0001-8572-5155

References

[1] E. Runge and E.K.U. Gross, Phys. Rev. Lett. **52**, 997 (1984).
[2] M.E. Casida, in *Recent Developments and Applications of Modern Density Functional Theory*, edited by J. Seminario (Elsevier, Amsterdam, 1996), volume 4 of *Theoretical and Computational Chemistry*, pp. 391–439.
[3] M. Petersilka, U.J. Gossmann, and E.K.U. Gross, Phys. Rev. Lett. **76**, 1212 (1996).
[4] C. Ullrich, *Time-Dependent Density-Functional Theory: Concepts and Applications*, Oxford Graduate Texts (OUP, Oxford, 2012).
[5] K. Burke, J. Werschnik, and E.K.U. Gross, J. Chem. Phys. **123**, 062206 (2005).
[6] D.J. Tozer and N.C. Handy, Phys. Chem. Chem. Phys. **2**, 2117 (2000).
[7] R.J. Cave, F. Zhang, N.T. Maitra, and K. Burke, Chem. Phys. Lett. **389**, 39 (2004).
[8] D.J. Tozer, R.D. Amos, N.C. Handy, B.O. Roos, and L. Serrano-Andres, Mol. Phys. **97**, 859 (1999).
[9] A. Dreuw, J.L. Weisman, and M. Head-Gordon, J. Chem. Phys. **119**, 2943 (2003).
[10] A. Dreuw and M. Head-Gordon, Chem. Rev. **105**, 4009 (2005).
[11] T. Leininger, H. Stoll, H.-J. Werner, and A. Savin, Chem. Phys. Lett. **275**, 151 (1997).
[12] H. Iikura, T. Tsuneda, T. Yanai, and K. Hirao, J. Chem. Phys. **115**, 3540 (2001).
[13] R. van Leeuwen and E.J. Baerends, Phys. Rev. A **49**, 2421 (1994).
[14] D.J. Tozer and N.C. Handy, J. Chem. Phys. **109**, 10180 (1998).
[15] M.E. Casida and D.R. Salahub, J. Chem. Phys. **113**, 8918 (2000).
[16] Q. Wu, P.W. Ayers, and W. Yang, J. Chem. Phys. **119**, 2978 (2003).
[17] M. Seaton, Rep. Prog Phys. **46**, 167 (1983).
[18] M. van Faassen and K. Burke, J. Chem. Phys. **124**, 094102 (2006).
[19] A. Sommerfeld, Ann Phys. **356**, 1 (1916).
[20] R. Guérout, M. Jungen, and C. Jungen, J. Phys. B Atom. Mol. Opt. Phys. **37**, 3043 (2004).
[21] R. Guérout, M. Jungen, and C. Jungen, J. Phys. B Atom. Mol. Opt. Phys. **37**, 3057 (2004).
[22] I. D. Petsalakis, G. Theodorakopoulos, and R.J. Buenker, J. Chem. Phys. **119**, 2004 (2003).
[23] F. Merkt, Ann. Rev. Phys. Chem. **48**, 675 (1997).
[24] G. Herzberg, Ann. Rev. Phys. Chem. **38**, 27 (1987).
[25] A.I. Al-Sharif, R. Resta, and C.J. Umrigar, Phys. Rev. A **57**, 2466 (1998).
[26] M. van Faassen and K. Burke, Phys. Chem. Chem. Phys. **11**, 4437 (2009).
[27] A. Wasserman and K. Burke, Phys. Rev. Lett. **95**, 163006 (2005).

[28] M. van Faassen and K. Burke, Chem. Phys. Lett. **431**, 410 (2006).
[29] P. Ring and P. Schuck, *The Nuclear Many-Body Problem*, Physics and astronomy online library (Springer, New York, NY, 2004).
[30] J. Blaizot and G. Ripka, *Quantum Theory of Finite Systems* (MIT Press, Cambridge, MA, 1986).
[31] H. van Aggelen, Y. Yang, and W. Yang, Phys. Rev. A **88**, 030501 (2013).
[32] D. Peng, S.N. Steinmann, H. van Aggelen, and W. Yang, J. Chem. Phys. **139**, 104112 (2013).
[33] G.E. Scuseria, T.M. Henderson, and I.W. Bulik, J. Chem. Phys. **139**, 104113 (2013).
[34] Y. Yang, H. van Aggelen, S.N. Steinmann, D. Peng, and W. Yang, J. Chem. Phys. **139**, 174110 (2013).
[35] C.-M. Liegener, Chem. Phys. Lett. **90**, 188 (1982).
[36] S. Taioli, S. Simonucci, L. Calliari, and M. Dapor, Phys. Rep. **493**, 237 (2010).
[37] Y. Yang, H. van Aggelen, and W. Yang, J. Chem. Phys. **139**, 224105 (2013).
[38] Y. Yang, D. Peng, J. Lu, and W. Yang, J. Chem. Phys. **141**, 124104 (2014).
[39] Y. Yang, D. Peng, E.R. Davidson, and W. Yang, J. Phys. Chem. A **119**, 4923 (2015).
[40] D. Peng, H. van Aggelen, Y. Yang, and W. Yang, J. Chem. Phys. **140**, 18A522 (2014).
[41] H. van Aggelen, Y. Yang, and W. Yang, J. Chem. Phys. **140**, 18A511 (2014).
[42] D.J. Rowe, Rev. Mod. Phys. **40**, 153 (1968).
[43] T. Helgaker, P. Jørgensen, and J. Olsen, *Molecular Electronic-Structure Theory* (Wiley, Chichester, 2000).
[44] Q. Wu, A.J. Cohen, and W. Yang, Mol. Phys. **103**, 711 (2005).
[45] An in-house program for QM/MM simulations (http://www.qm4d.info).
[46] A.E. Kramida, Y. Ralchenko, J. Reader, and N.A. Team, NIST Atomic Spectra Database (version 5.0), 2012.
[47] M. van Faassen, A. Wasserman, E. Engel, F. Zhang, and K. Burke, Phys. Rev. Lett. **99**, 043005 (2007).